A Gallium-Labeled DOTA-α-Melanocyte–Stimulating Hormone Analog for PET Imaging of Melanoma Metastases

Sylvie Froidevaux, PhD[1]; Martine Calame-Christe, PhD[1]; Jochen Schuhmacher, PhD[2]; Heidi Tanner[1]; Rainer Saffrich, PhD[2]; Markus Henze, MD[2]; and Alex N. Eberle, PhD[1]

[1]Laboratory of Endocrinology, Department of Research, University Hospital and University Children's Hospital, Basel, Switzerland; and [2]Department of Diagnostic and Therapeutic Radiology, German Cancer Research Center, Heidelberg, Germany

Although ^{18}F-FDG PET is widely used for metastatic melanoma diagnosis, it is less accurate than desirable, particularly for small foci. Since both melanotic and amelanotic melanomas overexpress receptors for α-melanocyte–stimulating hormone (α-MSH; receptor name, melanocortin type 1 receptor [MC1R]), radiolabeled α-MSH analogs are potential candidates for melanoma diagnosis. The aim of this study was to develop a positron emitter–labeled α-MSH analog suitable for PET imaging of melanoma metastases. **Methods:** A short linear α-MSH analog, [Nle^4,Asp^5,D-Phe^7]-α-MSH$_{4–11}$ (NAPamide), was newly designed and conjugated to the metal chelator DOTA (1,4,7,10-tetraazacyclododecane-1,4,7,10-tetraacetic acid) to enable radiometal incorporation. Compared with our previously reported DOTA-α-MSH analog, DOTA-MSH$_{oct}$ ([DOTA-βAla^3,Nle^4,Asp^5,D-Phe^7,Lys^{10}]-α-MSH$_{3–10}$), the major modification lies in the conjugation of DOTA to the C-terminal end of the peptide via the ε-amino group of Lys^{11}, as opposed to the N-terminal α-amino group. After labeling with ^{111}In, ^{67}Ga, and the short-lived positron emitter ^{68}Ga, DOTA-NAPamide was characterized in vitro and in vivo using the mouse melanoma B16F1cell line. **Results:** DOTA-NAPamide exhibited an almost 7-fold higher MC1R binding potency as compared with DOTA-MSH$_{oct}$. In B16F1 melanoma-bearing mice, both ^{111}In-DOTA-NAPamide and ^{67}Ga-DOTA-NAPamide behaved more favorably than ^{111}In-DOTA-MSH$_{oct}$. Both radiopeptides exhibited higher tumor and lower kidney uptake leading to tumor-to-kidney ratios of the 4- to 48-h area under the curve that were 4.6 times (^{111}In) and 7.5 times (^{67}Ga) greater than that obtained with ^{111}In-DOTA-MSH$_{oct}$. In addition, the 4-h kidney uptake of ^{67}Ga-DOTA-NAPamide could be reduced by 64% by coinjection of 15 mg L-lysine, without affecting tumor uptake. Skin primary melanoma as well as lung and liver melanoma metastases could be easily visualized on tissue section autoradiographs after systemic injection of ^{67}Ga-DOTA-NAPamide. The melanoma selectivity of DOTA-NAPamide was confirmed by PET imaging studies using ^{68}Ga-DOTA-NAPamide. Tumor uptake was found to be highest when the smallest amount of peptide was administered. **Conclusion:** DOTA-NAPamide labeled with either ^{111}In or ^{67}Ga/^{68}Ga is in every way superior to ^{111}In-DOTA-MSH$_{oct}$ in murine models of primary and metastatic melanoma, which makes it a promising agent for melanoma targeting. High-contrast images obtained in PET studies with an experimental tumor model 1 h after injection augurs well for its clinical potential as an imaging tool.

Key Words: melanoma imaging; α-melanocyte–stimulating hormone; 1,4,7,10-tetraazacyclododecane-1,4,7,10-tetraacetic acid; ^{67}Ga/^{68}Ga; PET

J Nucl Med 2004; 45:116–123

Melanocortin type-1 receptors (MC1R) known to be overexpressed in isolated melanoma cells and melanoma tissues (*1–4*) represent one of the very few specific targets potentially useful for diagnosis and therapy of metastatic melanoma. In view of the increasing incidence and mortality rates for cutaneous melanoma (*5*), the difficulties in detecting metastatic deposits and their inherent resistance to conventional chemotherapy (*6*), there is an urgent need for new diagnostic and therapeutic protocols. The successful development of radiolabeled somatostatin analogs, which are now routinely used in the clinic to visualize somatostatin receptor–positive malignancies (*7*) and show great promise for treatment of patients with neuroendocrine tumors (*8*), prompted us and others to evaluate radiolabeled α-melanocyte–stimulating hormone (α-MSH) analogs for targeting MC1R on (metastatic) melanoma.

Preclinical and clinical trials based on α-MSH analogs labeled with either ^{18}F via attachment of *N*-succinimidyl 4-^{18}F-fluorobenzoate or ^{111}In after conjugation to the metal chelator diethylenetriaminepentaacetic acid (DTPA) showed that melanoma tumors can be targeted and visualized with radiolabeled α-MSH (*9*). However, high nonspecific accumulation of these compounds in tissues such as liver (*10*) known to be common sites of distant melanoma metastases prevented further clinical development of DTPA-α-MSH compounds. More recently, α-MSH analogs that incorporate ^{99m}Tc or ^{88}Re into their 3-dimensional structures were reported to exhibit favorable properties for melanoma imaging in a mouse model (*11*,*12*). Also, we and others

Received May 27, 2003; revision accepted Oct. 3, 2003.

For correspondence or reprints contact: Sylvie Froidevaux, PhD, Department of Research, Kantonsspital Basel, Hebelstrasse 20, CH-4031 Basel, Switzerland.

E-mail: sylvie.froidevaux@unibas.ch

developed a novel class of radiolabeled α-MSH analogs, consisting of either short linear (*13*) or rhenium-cyclized peptides (*14,15*) conjugated to the metal chelator 1,4,7,10-tetraazacyclododecane-1,4,7,10-tetraacetic acid (DOTA). These DOTA-α-MSH analogs are interesting candidates for various applications of melanoma targeting in nuclear oncology not only because of their good biodistribution profiles in melanoma-bearing mice after labeling with ^{111}In but also because they carry DOTA, which can hold 2^+- and 3^+-charged radiometals. However, the clinical potential of α-MSH analogs might be further increased if one could lower their accumulation in kidneys, which remained high despite substantial recent progress (*14*).

The encouraging results with DOTA-α-MSH analogs prompted us to develop a radiolabeled α-MSH peptide suitable for PET, which offers higher sensitivity and contrast resolution than SPECT, making it possible to visualize very small metastatic lesions, including tumor deposits in regional draining lymph nodes. As the positron emitter, we selected ^{68}Ga (half-life [$t_{1/2}$], 68 min; β^+, 88%), which is produced by a ^{68}Ge/^{68}Ga generator available at most PET centers and is not dependent on a cyclotron. Gallium as a radiometal is of even broader interest in nuclear medicine because it is also available as ^{67}Ga ($t_{1/2}$, 78 h), which is not only a γ-emitter useful for tumor diagnosis (γ-camera scintigraphy, SPECT) but also an emitter of Auger (0.1–8 keV) and conversion electrons (80–90 keV), making it attractive for internal radiotherapy (*16*). In this study, a new DOTA-α-MSH analog was designed, [Nle^4,Asp^5,D-Phe^7-Lys^{11}(DOTA)]-α-MSH$_{4–11}$ (DOTA-NAPamide), in which DOTA was conjugated to the C-terminal end of the peptide via the ε-amino group of Lys^{11}. Compared with our previously reported DOTA-MSH$_{oct}$, [DOTA-βAla^3,Nle^4,Asp^5,D-Phe^7,Lys^{10}]-α-MSH$_{3–10}$ (*13*), DOTA-NAPamide differs mainly by (a) the position of DOTA in the peptide (C-terminal vs. N-terminal end), (b) the net charge (charge +1 vs. +2), and (c) the reintroduction of Gly at position 10 (as in native α-MSH peptide, where it was shown to play some role in MC1R affinity (*17*)). Since tumor uptake is closely related to receptor affinity, whereas kidney clearance is known to be influenced by the charge of molecules, we expected DOTA-NAPamide to exhibit a more favorable biodistribution profile than DOTA-MSH$_{oct}$, particularly with regard to the tumor-to-kidney uptake ratio. DOTA-NAPamide was labeled with ^{67}Ga/^{68}Ga or with ^{111}In for direct comparison with ^{111}In-DOTA-MSH$_{oct}$ and characterized in vitro and in vivo using the B16F1 mouse melanoma cell line.

MATERIALS AND METHODS

Peptides and Radioligands

α-MSH was a gift from Novartis and [Nle^4,D-Phe^7]-α-MSH (NDP-MSH) was purchased from Bachem. The α-MSH analogs [βAla^3,Nle^4,Asp^5,D-Phe^7,Lys^{10}]-α-MSH$_{3–10}$ (MSH$_{oct}$) and [Nle^4,Asp^5,D-Phe^7]-α-MSH$_{4–11}$ (NAPamide) (Fig. 1) were synthesized in our laboratory using the continuous-flow technology and Fmoc (9-fluorenylmethoxycarbonyl) strategy. Conjugation of partially protected DOTA ([4,7,10-tri(carboxymethyl-tert-butyl ester)]-1,4,7,10-tetraazacyclododecane-1-acetate) to MSH$_{oct}$ was performed as previously described (*13*). NAPamide was conjugated to DOTA by adding deprotected peptide (4.5 μmol) dissolved in *N,N′*-diisopropylethylamine (1.5 μL)/dimethylformamide (DMF; 100 μL) to DOTA (4.5 μmol) preincubated for 10 min with 0-[7-azabenzotriazole-1-yl]-1,1,3,3-tetramethyluronium hexafluorophosphate (5.4 μmol)/DMF (300 μL). After a 1-h incubation at room temperature and precipitation of the peptide in ice-cold diethylether, deprotection of DOTA was performed by adding 3.6 mL trifluoroacetic acid (TFA), 0.2 mL thioanisole, 0.18 mL water, and 0.02 mL 1,2-ethanedithiol. After stirring for 4 h, the deprotected DOTA-peptide was precipitated with ice-cold diethylether and resuspended in 10% acetic acid before purification by reversed-phase high-performance liquid chromatography (RP-HPLC). The major peak was collected and analyzed by electrospray ionization mass spectrometry.

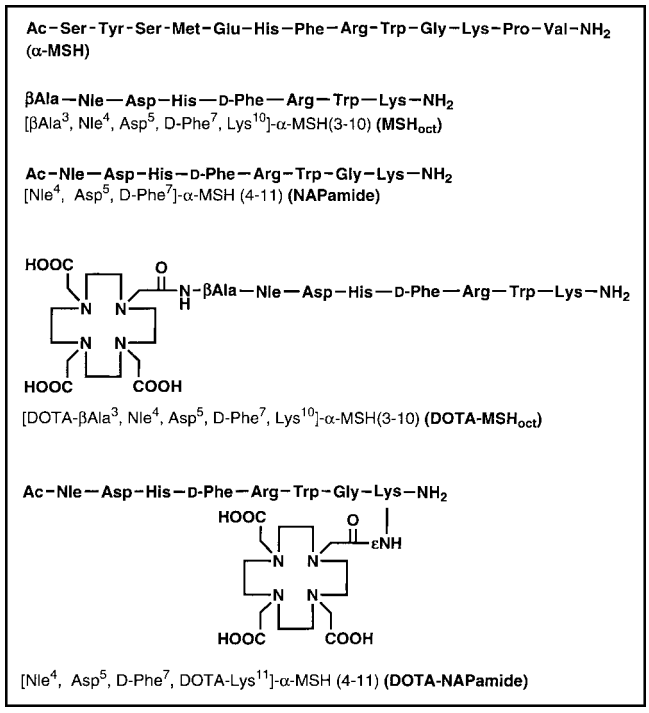

FIGURE 1. Structure of α-MSH, MSH$_{oct}$, NAPamide, and corresponding DOTA conjugates.

Incorporation of ^{111}In and ^{67}Ga into DOTA-peptides was performed by adding 92.5 MBq $^{111}InCl_3$ (Mallinckrodt) or $^{67}GaCl_3$ (Mallinckrodt or MDS Nordion) to DOTA-peptide (10 nmol) dissolved in 53 μL acetate buffer (0.4 mol/L, pH 5) containing 2 mg gentisic acid. After a 30-min incubation at 95°C, the purity of the resulting radioligand was assessed by RP-HPLC on a Jasco PU-980 chromatography system connected to a Radiomatic 500TR LB506C1 γ-detector (Packard) and a Spherisorb ODS2/5-μm column under the following conditions: eluent A = 0.1% TFA in water; eluent B = 0.1% TFA in acetonitrile; gradient = 0–2 min, 96% A; 2–22 min, 96%–45% A; 22–30 min, 45%–25% A; 30–32 min, 25% A; 32–34 min, 25%–96% A; flow rate, 1.0 mL/min. When necessary, the radiolabeled DOTA-peptide was purified on a small reversed-phase cartridge (Sep-Pak C_{18}; Waters Corp.)

using ethanol as solvent. The ethanol fraction containing the purified radiopeptide was evaporated under argon at 70°C. The specific activity of the radioligands was always >7.4 GBq/μmol.

^{68}Ga labeling was performed as followed. ^{68}Ga was obtained in 0.5 mL 0.5N HCl from a ^{68}Ge/^{68}Ga radionuclide generator. After addition of 1.5 μL 1 mmol/L Ga^{3+}, the mixture was evaporated to dryness and redissolved in 500 μL acetate buffer (0.1 mol/L, pH 4.8) to which DOTA-NAPamide (5 μL, 3.2 nmol) was added. The mixture was heated for 15 min at 90°C and ^{68}Ga-DOTA-NAPamide was purified on an RP-cartridge as described above for ^{67}Ga/^{111}In-labeled DOTA-peptides. More than 98% radioactivity was incorporated into DOTA-NAPamide as checked by paper chromatography (Whatman no. 1; methanol-to-water ratio, 55:45).

Iodination of NDP-MSH was performed by the chloramine-T method. NDP-MSH (3 μg) was mixed with $Na^{125}I$ (37 MBq; Amersham) in 50 μL phosphate-buffered saline (PBS; 0.3 mol/L, pH 7.2), followed by the addition of 10 μL chloramine-T (2 mg/mL; Merck). After incubation for 5 min, the reaction was stopped with 500 μL dithiothreitol (DTT; 20 mg/mL) and the monoiodinated peptide was purified on a syringe packed with 0.25 g Spherisorb ODS/10-μm reversed-phase silica (Phase Separations, Inc.) using a stepwise gradient of aqueous methanol containing 1% TFA. The fractions containing ^{125}I-NDP-MSH were supplemented with DTT (1.5 mg/mL) and stored at −20°C. Before each binding experiment, an additional purification was performed by RP-HPLC.

Cell Culture

The mouse B16F1 melanoma cell line (*18*) was cultured in modified Eagle's medium supplemented with 10% heat-inactivated fetal calf serum, 2 mmol/L L-glutamine, 1% nonessential amino acids, 1% vitamin solution, 50 units/mL penicillin, and 50 μg/mL streptomycin (all from GIBCO) at 37°C in a humidified atmosphere of 95% air/5% CO_2. For expansion or experiments, the cells were detached with 0.02% ethylenediaminetetraacetic acid in PBS (150 mmol/L, pH 7.2–7.4).

In Vitro Binding Assay

Competitive binding experiments were performed by incubating MC1R-expressing B16F1 cells in microplates with the radioligand ^{125}I-NDP-MSH and a series of dilutions of competitor peptides (from 1×10^{-6} to 1×10^{-12} mol/L) at 15°C for 3 h as described previously (*19*). Values of the inhibitory concentration yielding 50% binding (IC_{50}) were calculated using GraphPad Prism software.

Biodistribution Experiments and Autoradiography

All animal experiments were performed in compliance with the Swiss regulation for animal treatment.

Female B6D2F1 mice (C57Bl/6 × DBA/2 F1 hybrids, breeding pairs obtained from IFFA-CREDO) were implanted subcutaneously with 0.5 million B16F1 cells to generate a primary skin melanoma. One week later, radioligand (185 kBq, except where otherwise stated), diluted in NaCl, 0.1% bovine serum albumin, pH 7.5, was injected intravenously in the lateral tail vein in a volume of 200 μL. To determine nonspecific uptake, 50 μg α-MSH was coinjected with the radioligand. To reduce kidney uptake, 15 mg L-lysine (GIBCO) was coinjected with the radioligand. The animals were killed at the indicated time points; organs and tissues of interest were dissected and rinsed of excess blood, weighed, and assayed for radioactivity in a γ-counter. The percentage of injected dose per gram (%ID/g) was calculated for each tissue. The total counts injected per animal were calculated by extrapolation from counts of a standard taken from the injected solution for each animal.

For tissue autoradiography experiments, B6D2F1 mice with a primary or metastatic melanoma were injected with 740 kBq radioligand. Melanoma metastases were induced by intravenous injection of $2–5 \times 10^4$ B16F1 cells preincubated for 2 d with 10–100 units/mL interferon-γ (Pharmingen) to increase their metastatic potential. Mice were killed 4 h after radioligand injection and tissues of interest were removed and immediately fixed in isopentane cooled in nitrogen liquid. Frozen sections (100-μm thick) were cut using a Microm HM 560 microtome refrigerated at −25°C and transferred onto glass slides precooled on dry ice. The tissue sections were placed in a lyophilizator (LDC-1M; Kühner) and dried completely overnight before exposure to a Molecular Dynamics Storage Phosphor Plate for 1–2 d. The phosphor plate was scanned with a Molecular Dynamics PhosphorImager using ImageQuant to obtain digital autoradiographs that were further processed in Adobe Photoshop 5.0. After autoradiography, dehydrated tissue sections were scanned (model EU-35; Seiko Epson Corp.) and processed using Adobe Photoshop 5.0 and superimposed on the autoradiographs.

PET Studies

B6D2F1 female mice bearing a B16F1 melanoma in their right flank were injected intravenously with ^{68}Ga-DOTA-NAPamide. After time periods ranging from 0.5 to 3 h, animals were killed and imaged with a 20-min emission and a 10-min transmission scan on a Siemens ECAT EXACT HR^+ scanner (*20*). Images were taken in the 3-dimensional mode, corrected for scatter and attenuation and reconstructed iteratively from a 256 × 256 matrix for viewing transaxial, coronal, and sagittal slices of 2.3 mm in thickness (*21*). Pixel size was 1.2 mm and transaxial resolution was 4.2 mm. Subsequently, tumor and kidneys were removed, weighed, and counted for ^{68}Ga radioactivity in a γ-counter.

Analysis of Data

Unless otherwise stated, results are expressed as mean ± SEM. Statistical evaluation was performed using the 1- or 2-way ANOVA test. When significant overall effects were obtained by ANOVA, multiple comparisons were made with the Bonferroni correction. $P < 0.05$ was considered to indicate a statistically significant difference. The area under the curve (AUC) was calculated with GraphPad Prism software for the indicated period of time, using the mean tissue uptake value at each time point.

RESULTS

Synthesis of DOTA-NAPamide and DOTA-MSH_{oct}

The synthesis of NAPamide and its conjugation to the metal chelator DOTA was performed as described in the Materials and Methods. DOTA-NAPamide was obtained in >99% purity and in 15% overall yield (after RP-HPLC purification). Mass spectrometry confirmed the expected molecular weight for DOTA-NAPamide (experimental, 1485.5; calculated, 1485.7). Data concerning the synthesis of DOTA-MSH_{oct} corresponded to those previously reported (*13*).

Receptor Binding

The MC1R binding affinity of NAPamide, MSH_{oct}, and their DOTA conjugates were assessed by competition bind-

TABLE 1
MC1R Affinity of α-MSH Analogs

MSH analog	IC_{50}* (nmol/L)
α-MSH	1.70 ± 0.28
MSH_{oct}	1.25 ± 0.08
NAPamide	0.27 ± 0.07
DOTA-MSH_{oct}	9.21 ± 1.27
DOTA-NAPamide	1.37 ± 0.35

*MC1R affinity of α-MSH analogs was assessed by competition binding experiments with B16F1 cells and ^{125}I-NDP-MSH as radioligand (mean ± SEM; n = 3–9).

Statistics: α-MSH vs. NAPamide, $P < 0.05$; MSH_{oct} vs. NAPamide, $P > 0.05$; DOTA-MSH_{oct} vs. DOTA-NAPamide, $P < 0.001$.

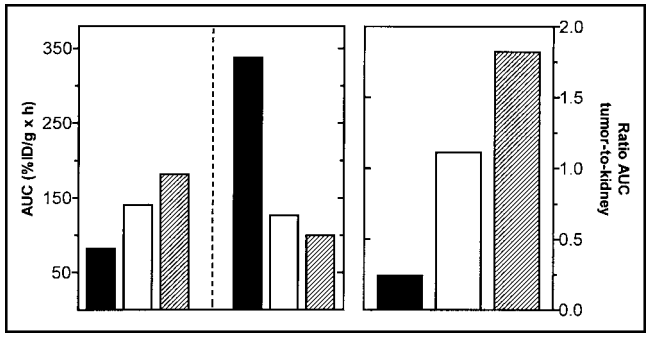

FIGURE 2. Tumor versus kidney uptake. Radiolabeled DOTA-α-MSH analogs (■, ^{111}In-DOTA-MSH_{oct}; □, ^{111}In-DOTA-NAPamide; ▨, ^{67}Ga-DOTA-NAPamide) were injected into melanoma-bearing mice and radioactivity accumulated in tumor and kidney was measured 4, 24, and 48 h after injection. Results are expressed as tumor AUC (left), kidney AUC (middle), and tumor-to-kidney ratios of AUC (right) (n = 8).

ing experiments with B16F1 cells. Table 1 lists the IC_{50} values in comparison with that of the natural ligand α-MSH as control. Although both DOTA-α-MSH analogs displayed favorable receptor affinity (low nanomolar range), DOTA-NAPamide exhibited higher binding potency than DOTA-MSH_{oct} (6.7-fold). It was noted that attachment of DOTA to the N- or C-terminal end of the peptide induced a comparable moderate decrease of MC1R binding affinity, demonstrating that DOTA can be conjugated to either of the 2 peptide ends without compromising receptor affinity.

Biodistribution in Melanoma-Bearing Mice and Effect of Quantity of Injected Peptide

Table 2 presents the 4- to 48-h tissue distribution of DOTA-NAPamide labeled with ^{111}In or ^{67}Ga (185 kBq; specific activity, >7.4 GBq/μmol). The 4-h tissue distribution of ^{111}In-DOTA-MSH_{oct} (*13*) is included as a reference. Compared with ^{111}In-DOTA-MSH_{oct}, ^{111}In-DOTA-NAPamide showed a more favorable behavior as indicated by higher tumor (1.75×) and lower kidney uptake (2.7×) 4 h after injection (Table 2). The same is true for all later time points (for 24- or 48-h biodistribution data for ^{111}In-DOTA-MSH_{oct}, see (*13*)). Accordingly, the tumor-to-kidney ratio of the AUC calculated for the time period 4–48 h was almost 5 times greater for ^{111}In-DOTA-NAPamide (Fig. 2). Although blood clearance was somewhat slower for ^{111}In-DOTA-NAPamide, the 4-h uptake in normal tissues (except

TABLE 2
Tissue Distribution at 4, 24, and 48 Hours After Injection

	Time after injection (h)						
	4			24		48	
Tissue	^{111}In-DOTA-MSH_{oct}	^{111}In-DOTA-NAPamide	^{67}Ga-DOTA-NAPamide	^{111}In-DOTA-NAPamide	^{67}Ga-DOTA-NAPamide	^{111}In-DOTA-NAPamide	^{67}Ga-DOTA-NAPamide
Blood	0.03 ± 0.00*	0.12 ± 0.01	0.26 ± 0.03*	0.01 ± 0.00	0.06 ± 0.01†	0.00 ± 0.00	0.02 ± 0.00
Muscle	0.03 ± 0.01	0.05 ± 0.01	0.05 ± 0.01	0.01 ± 0.00	0.02 ± 0.00	0.01 ± 0.00	0.02 ± 0.00
Liver	0.41 ± 0.02	0.43 ± 0.04	0.28 ± 0.02*	0.30 ± 0.02	0.25 ± 0.02	0.23 ± 0.00	0.23 ± 0.02
Kidney	13.5 ± 1.12*	5.06 ± 0.32	3.98 ± 0.10	2.65 ± 0.36	2.04 ± 0.17	1.46 ± 0.08	1.24 ± 0.09
Spleen	0.15 ± 0.01	0.15 ± 0.01	0.17 ± 0.02	0.10 ± 0.01	0.14 ± 10.01	0.11 ± 0.01	0.15 ± 0.02
Lung	0.10 ± 0.01	0.09 ± 0.01	0.20 ± 0.03*	0.05 ± 0.01	0.09 ± 0.01	0.03 ± 0.00	0.06 ± 0.01
Small intestine	0.11 ± 0.03	0.07 ± 0.01	0.16 ± 0.02‡	0.04 ± 0.00	0.13 ± 0.02‡	0.03 ± 0.00	0.12 ± 0.02‡
Heart	0.03 ± 0.00	0.05 ± 0.01	0.09 ± 0.01*	0.03 ± 0.01	0.03 ± 0.00	0.02 ± 0.00	0.03 ± 0.00
Bone	0.08 ± 0.01	0.13 ± 0.03	0.36 ± 0.05*	0.18 ± 0.04	0.28 ± 0.03	0.04 ± 0.01	0.27 ± 0.04*
Pancreas	0.03 ± 0.00	0.04 ± 0.00	0.09 ± 0.01*	0.02 ± 0.00	0.06 ± 0.01*	0.02 ± 0.00	0.05 ± 0.01‡
Skin	0.10 ± 0.02†	0.18 ± 0.04	0.19 ± 0.02	0.05 ± 0.01	0.11 ± 0.02	0.07 ± 0.01	0.08 ± 0.01
Stomach	0.10 ± 0.02	0.09 ± 0.02	0.11 ± 0.01	0.08 ± 0.01	0.11 ± 0.01	0.05 ± 0.01	0.15 ± 0.05
Tumor	4.31 ± 0.30*	7.56 ± 0.51	9.43 ± 1.06†	2.32 ± 0.28	3.10 ± 0.36	1.16 ± 0.06	1.61 ± 0.20

*$P < 0.001$ vs. ^{111}In-DOTA-NAPamide.

†$P < 0.05$ vs. ^{111}In-DOTA-NAPamide.

‡$P < 0.01$ vs. ^{111}In-DOTA-NAPamide.

^{111}In-DOTA-NAPamide, ^{67}Ga-DOTA-NAPamide, or ^{111}In-DOTA-MSH_{oct} as reference compound was injected to melanoma-bearing mice and tissue-associated radioactivity was measured 4, 24, and 48 h after injection. Results are expressed as %ID/g (mean ± SEM; n = 4–8).

kidney) was low and was similar for the 2 radioligands (only skin uptake was slightly higher for ^{111}In-DOTA-NAPamide) (Table 2). Replacement of ^{111}In with ^{67}Ga had a positive overall influence on the performance of DOTA-NAPamide; tumor uptake in particular was increased and kidney uptake was reduced, leading to a 1.65-fold increase in the tumor-to-kidney ratio of the AUC (Fig. 2). Kidney uptake of ^{67}Ga-DOTA-NAPamide could be further specifically reduced by L-lysine administration: The 4-h renal uptake decreased by 64% when 15 mg L-lysine were coinjected with the radioligand, whereas radioactivity in tumor and excretory organs such as liver and small intestine was not affected (not shown). Coinjection of an excess of α-MSH to block the MC1R reduced the 4-h tumor uptake of ^{111}In- or ^{67}Ga-DOTA-NAPamide by >80%, indicating that DOTA-NAPamide is taken up by melanoma through a receptor-mediated process (not shown). Thus, DOTA-NAPamide labeled with ^{111}In or ^{67}Ga displayed a more favorable overall biodistribution profile than the previously reported DOTA-α-MSH analog, particularly regarding kidney retention.

To study the effect of the quantity of injected peptide on the tissue distribution, melanoma-bearing mice were injected with a mixture of Ga-DOTA-NAPamide/^{67}Ga-DOTA-NAPamide containing variable quantities of peptide (20, 170, or 420 pmol) but a constant amount of radioactivity (185 kBq). Radioactivity uptake in normal tissues and melanoma was monitored 4 h later and results are shown in Figure 3. Tumor uptake was dramatically affected by the quantity of peptide administered: A 5-fold decrease was observed in mice injected with 420 pmol as compared with that obtained in animals receiving the lowest dose, 20 pmol. Kidney uptake was much less influenced by peptide dosage since it was only reduced by 1.4-fold by increasing the quantity from 20 to 420 pmol. Uptake in other tissues remained unchanged regardless of the quantity of peptide. Taken together, these results clearly indicate that tumor uptake and, to a much lesser extent, kidney uptake were dependent on the amount of radiopeptide injected; the highest tumor-to-kidney uptake ratio was obtained with the lowest quantity tested.

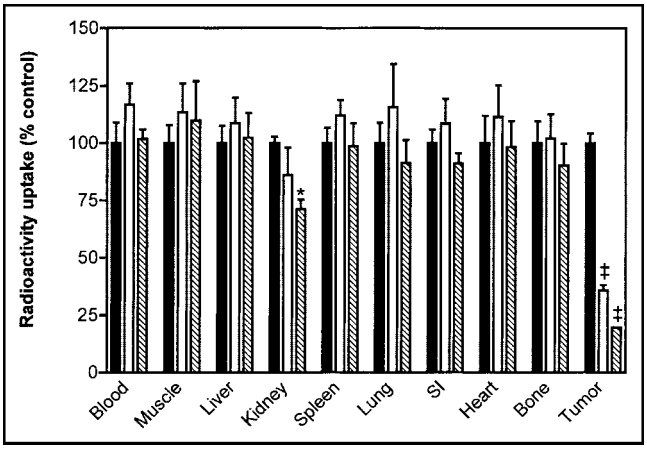

FIGURE 3. Effect of quantity of peptide on tissue distribution. Melanoma-bearing mice were injected with 185 kBq ^{67}Ga-DOTA-NAPamide (9.25 GBq/μmol) supplemented with various amounts of nonradioactive Ga-DOTA-NAPamide to obtain total peptide quantity per mouse of 20 pmol (■), 170 pmol (□), or 420 pmol (▨). Radioactivity accumulated in main tissues was measured 4 h after injection and results are expressed as percentage of uptake (%ID/g) observed after injection of 20 pmol (mean ± SEM, n = 3 or 4). *$P < 0.05$, ‡$P < 0.001$ vs. 20 pmol. SI = small intestine.

Autoradiography of Primary and Metastatic Melanoma

^{67}Ga-DOTA-NAPamide was injected into mice with primary skin melanoma or metastatic lung or liver melanoma, and sections of tissues showing macroscopic melanoma lesions were examined by autoradiography. Autoradiographs and corresponding tissue section scans are shown in Figure 4. The boundary between the malignant lesion and the normal tissue was clearly visible by macroscopic examination making staining unnecessary. All macroscopically identified melanoma lesions (amelanotic and melanotic lesions) in the lung, liver, or skin sections could be imaged on autoradiographs, confirming the selective accumulation of ^{67}Ga-DOTA-NAPamide. Uptake in the primary lesions (skin) and metastatic lesions (lung) was found to be quantitatively similar (metastatic melanoma uptake expressed as % [mean ± SEM; n = 5] of that obtained for primary skin melanoma = 96.5% ± 4.8%). Moreover, the diffusion of the radiopeptide throughout the tumor was good as indicated by uniform distribution of radioactivity. Thus, tissue autoradiography confirmed the favorable biodistribution profile of ^{67}Ga-DOTA-NAPamide and demonstrated its potential for diagnosis of metastatic melanoma.

PET Imaging of Melanoma-Bearing Mice with ^{68}Ga-DOTA-NAPamide

Melanoma-bearing mice were injected with ^{68}Ga-DOTA-NAPamide and imaged with a PET scanner at 0.5, 1, 2, and 3 h after injection. Based on the data with ^{67}Ga (Fig. 3), the quantity of ^{68}Ga-DOTA-NAPamide administered to mice (40 pmol) was kept as low as possible by taking into account the specific activity of ^{68}Ga-DOTA-NAPamide and the dose of radioactivity required for a 3-h PET scan. As early as 0.5 h after injection, only tumor, kidney, bladder, and, to a much lower extent, heart were visible, demonstrating a rapid tumor uptake and a fast blood clearance via kidneys. Thereafter, heart and kidney uptake decreased, whereas tumor uptake remained unchanged. The optimum tumor-to-normal tissue contrasts were obtained 1 h after injection (Figs. 5A and 5B). The kinetic of tumor and kidney uptake is better illustrated in the biodistribution data showing a constant amount of radioactivity in the tumor during the period of observation (0.5–3 h), whereas that which accumulated in the kidneys dropped by 35% from 0.5 to 1 h after injection before reaching a stable level lasting until the end of the experiment (3 h) (Fig. 5C). The tumor uptake of 7 %ID/g 3 h after injection of 40 pmol ^{68}Ga-

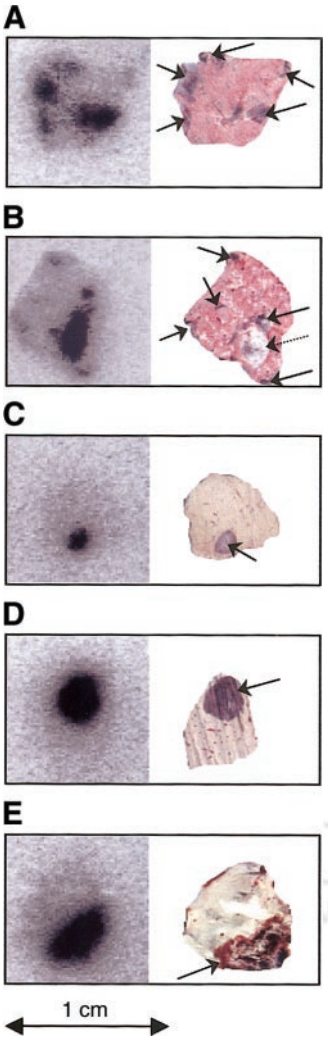

FIGURE 4. Autoradiographs of tissue sections from primary and metastatic melanoma. (A) Lung with melanotic melanoma metastases. (B) Lung with melanotic or amelanotic melanoma metastases. (C and D) Liver with melanotic melanoma metastases. (E) Primary melanoma with surrounding skin tissue. ^{67}Ga-DOTA-NAPamide was injected into tumor-bearing mice. Primary skin melanoma and tissues showing macroscopic metastases were collected 4 h later and immediately fixed. After sectioning, tissues were exposed to Molecular Dynamics Storage Phosphor Plate (left) and later were exposed to scanner (right). Arrows indicate amelanotic (dotted arrow) or melanotic (solid arrows) metastatic nodules.

DOTA-NAPamide fits well with that obtained with ^{67}Ga-DOTA-NAPamide (9.43 %ID/g 4 h after injection of about 20 pmol) (Table 2).

DISCUSSION

Diagnostic accuracy of ^{18}F-FDG PET in patients with melanoma is less than desirable, particularly for small tumor foci and initial regional staging (*22*). Another limitation is that some melanoma cells do not use glucose but use other substrates for energy supply, which makes them undetectable with ^{18}F-FDG (*23*). Therefore, the main goal of this project was to develop a melanoma-specific radiolabeled α-MSH analog suitable for PET imaging of melanoma metastases in patients. In view of the favorable characteristics of the positron emitter ^{68}Ga, including its production from a generator and its short half-life (68 min), we focused on the development of a Ga-labeled α-MSH analog. An additional advantage of gallium is that it is also available as ^{66}Ga and ^{67}Ga, 2 radiometals of interest in nuclear medicine. ^{66}Ga is a cyclotron-produced positron emitter with a longer half-life than ^{68}Ga (9.5 h), which may therefore also be suitable for PET imaging and possibly complements ^{68}Ga when lesions in the region of the urinary tract are suspected. ^{67}Ga is suited for tumor diagnosis and potentially for internal radiotherapy. Therefore, a Ga-labeled α-MSH analog would provide a polyvalent tool for the clinical management of melanoma, including PET imaging. We selected the

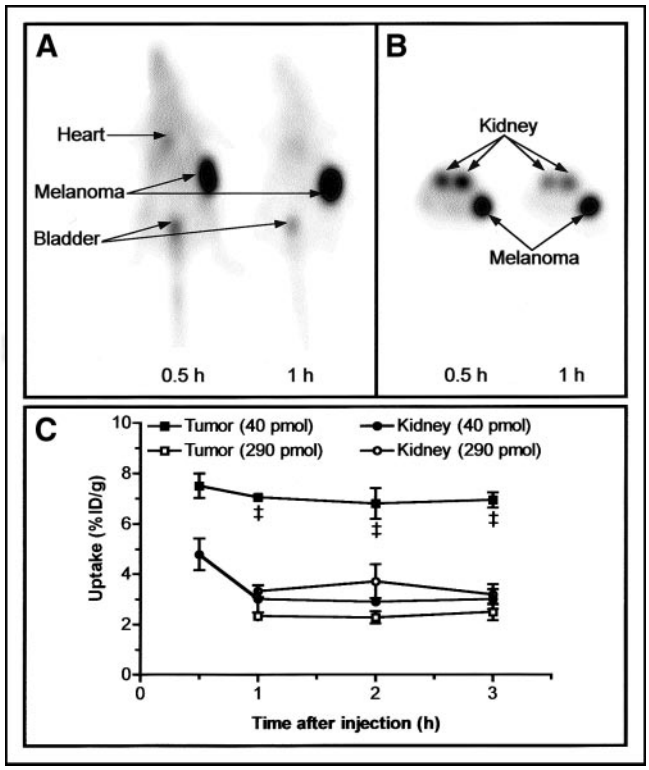

FIGURE 5. PET imaging of melanoma-bearing mice with ^{68}Ga-DOTA-NAPamide. (A and B) Scatter- and attenuation-corrected PET images of melanoma-bearing mice. ^{68}Ga-DOTA-NAPamide (50.1 GBq/μmol; 40 pmol) was injected into mice implanted in right flank with B16F1 melanoma and imaged at 0.5, 1, 2, and 3 h after injection ($n = 2$): coronal image (A) and transaxial image (B) of mice 0.5 h (tumor weight, 300 mg) and 1 h (tumor weight, 344 mg) after injection. Only melanoma, kidneys, bladder, and, to a lesser extent, heart are detectable. No further background reduction could be observed at later time points. (C) Kinetics of tumor and kidney uptake. Melanoma-bearing mice were injected with either 40 pmol (50.1 GBq/μmol) or 290 pmol (16.5 GBq/μmol) ^{68}Ga-DOTA-NAPamide. Melanoma and kidneys were collected 0.5, 1, 2, and 3 h after injection and radioactivity was measured in γ-counter. Results are expressed as %ID/g tissue (mean ± SEM; $n = 2–4$). ‡$P < 0.001$ vs. 290 pmol.

metal chelator DOTA to chelate gallium since it is capable of forming stable complexes with various 3^+-charged radiometals (*24*,*25*), including gallium, as demonstrated by the successful development of Ga-labeled DOTA-somatostatin analogs (*26*,*27*). A newly designed DOTA-α-MSH analog, DOTA-NAPamide, was used as vector. The latter differs from other DOTA-α-MSH analogs reported so far (*13*–*15*) by the C-terminal position of DOTA. We hypothesized that the conjugation of DOTA to the C-terminal end of the peptide via the ε-amino group of Lys^{11} would favor renal excretion by neutralizing the positive charge of the ε-amino group in the peptide. Diminution of the positive charge of molecules was reported to be associated with a reduction in both glomerular filtration and tubular reabsorption and, thereby, kidney accumulation (*28*–*31*). Moreover, Akisawa et al. demonstrated that renal uptake of ^{111}In-[DTPA-D-Phe^1]octreotide was enhanced by substitution of D-Phe^1 with Lys but was reduced when D-Phe^1 was replaced by Asp, pointing out the influence of charge on kidney retention of chelator-peptide conjugates (*32*). In comparison with DOTA-MSH_{oct}, a Gly residue was introduced at position 10 to lengthen the distance between the acidic DOTA molecule and the sequence 6–9 of the peptide known to be critical for receptor recognition. Additionally, a Gly residue at this position appears to increase receptor affinity (*17*).

Competition binding experiments with melanoma B16F1 cells revealed that DOTA-NAPamide displayed much higher MC1R binding potency than DOTA-MSH_{oct}, indicating that the ε-amino group of Lys^{11} is suitable for DOTA coupling. This is in agreement with reported data showing that conjugation of 4-fluorobenzoate (*33*) or 2.3-dihydroxy-(2*S*)-propyl (*34*) to Lys^{11} via its ε-amino group did not compromise receptor affinity. In accordance with receptor binding data, tumor uptake of ^{111}In-DOTA-NAPamide was higher than that of ^{111}In-DOTA-$MSH_{oct,}$ when tested in the same melanoma-bearing mouse model. We also observed decreased kidney accumulation of ^{111}In-DOTA-NAPamide compared with ^{111}In-DOTA-MSH_{oct}. To our knowledge, the amount of ^{111}In accumulation in kidneys was the lowest reported so far with DOTA-α-MSH analogs (*14*,*15*). The tumor-to-kidney ratio of radioactivity uptake could be further increased by incorporating ^{67}Ga instead of ^{111}In; the positive influence of gallium on biodistribution profiles of DOTA peptides has already being reported (*26*) and might be related to differences in the coordination chemistry of metals (*35*). As with most radiopeptides (*12*,*36*,*37*), renal accumulation of ^{67}Ga-DOTA-NAPamide could be decreased by coinjection of L-lysine without affecting tumor retention. Unexpectedly, though the positive charge of the lysine residue was neutralized in DOTA-NAPamide, the level of reduction (64%) paralleled or even exceeded that obtained with other radiopeptides in rodents (40%–52%) (*12*,*36*,*37*). This indicates that the residual renal accumulation of DOTA-NAPamide may very likely be further reduced in patients by coadministration of the standard cocktail of basic amino acids. The suitability of gallium-labeled DOTA-NAPamide for metastasis imaging was confirmed by tissue autoradiography. After injection of ^{67}Ga-DOTA-NAPamide, all macroscopically detectable melanoma lesions were indeed visible on sections of liver, lung, or skin exhibiting melanotic or amelanotic melanoma tumors. This result is particularly relevant with regard to the prevalence of pulmonary and liver metastases in cutaneous melanoma patients (*10*). The excellent selectivity of gallium-labeled DOTA-NAPamide was also demonstrated by PET studies using ^{68}Ga as the positron emitter. In summary, these results indicate that coupling of DOTA to Lys^{11}, as opposed to the usual N-terminal amino acid, might improve biologic performance of α-MSH analogs, particularly regarding renal clearance.

Our study on the role of the quantity of injected peptide on the tumor-to-background ratio revealed that tumor uptake was dramatically affected by the dose of peptide, whereas nontarget tissue uptakes were not or very moderately modified (kidney). A 5-fold increase in tumor uptake was observed by reducing the peptide dosage from 420 to 20 pmol, although kidney retention decreased by only 1.4-fold. This demonstrates the importance of the specific activity of the radiopeptide: The amount of administered peptide can be kept low only if the specific activity is high, resulting in a maximum tumor-to-background ratio. The dose-dependent tumor uptake of radiopeptide may explain the lower accumulation of ^{111}In-DOTA-NAPamide (7.6 %ID/g at 4 h) in melanoma compared with that reported for a cyclic DOTA-α-MSH analog (^{111}In-labeled compound 6, 17.4 %ID/g at 4 h) (*14*), although both peptides exhibit similar MC1R affinity. The amount of ^{111}In-DOTA-NAPamide injected per animal was about 20 pmol—that is, almost 500-fold more than the quantity of ^{111}In-labeled compound 6 (0.043 pmol). Ongoing studies are focusing on improving the specific activity of ^{111}In-DOTA-NAPamide to allow administration of a lower dosage of radiopeptide. A similar investigation has been reported in rats using a radiolabeled DOTA-somatostatin analog but with somewhat different results (*38*). In that study, uptake in tumor as a function of the dose of injected radiopeptide followed a bell-shape curve, the highest value being observed after administration of 330 pmol. The reason for this apparent discrepancy between the 2 studies is unclear but may be related to the presence of local endogenous ligand (for example, somatostatin) which competes with the radiopeptide for binding to the targeted receptor.

CONCLUSION

DOTA-NAPamide labeled with ^{111}In, ^{67}Ga, or ^{68}Ga exhibits more favorable overall performance than ^{111}In-DOTA-MSH_{oct} in murine models of primary and metastatic melanoma. The major improvement lies in reduced kidney retention, which may result from the position of DOTA in the peptide. The high tumor selectivity of gallium-labeled DOTA-NAPamide, which enables applications in diagnosis

and therapy, makes DOTA-NAPamide a promising tool for the clinical management of melanoma. A pilot clinical study aimed at examining its performance for PET imaging of melanoma metastases is planned for the near future.

ACKNOWLEDGMENTS

We thank Dr. Joyce Baumann for her critical review of the manuscript. This work was supported by the Swiss Cancer League and the Swiss National Science Foundation.

REFERENCES

1. Jiang J, Sharma SD, Fink JL, Hadley ME, Hruby VJ. Melanotropic peptide receptors: membrane markers of human melanoma cells. *Exp Dermatol.* 1996;5: 325–333.
2. Ghanem GE, Comunale G, Libert A, Vercammen-Grandjean A, Lejeune FJ. Evidence for alpha-melanocyte-stimulating hormone (alpha-MSH) receptors on human malignant melanoma cells. *Int J Cancer.* 1988;41:248–255.
3. Siegrist W, Solca F, Stutz S, et al. Characterization of receptors for alpha-melanocyte-stimulating hormone on human melanoma cells. *Cancer Res.* 1989; 49:6352–6358.
4. Bagutti C, Oestreicher M, Siegrist W, Oberholzer M, Eberle AN. Alpha-MSH receptor autoradiography on mouse and human melanoma tissue sections and biopsies. *J Recept Signal Transduct Res.* 1995;15:427–442.
5. Dennis LK. Analysis of the melanoma epidemic, both apparent and real: data from the 1973 through 1994 surveillance, epidemiology, and end results program registry. *Arch Dermatol.* 1999;135:275–280.
6. Rossi CR, Foletto M, Vecchiato A, Alessio S, Menin N, Lise M. Management of cutaneous melanoma M0: state of the art and trends. *Eur J Cancer.* 1997;33: 2302–2312.
7. Krenning EP, Kwekkeboom DJ, Bakker WH, et al. Somatostatin receptor scintigraphy with [^{111}In-DTPA-D-Phe^{1}]- and [^{123}I-Tyr^{3}]-octreotide: the Rotterdam experience with more than 100 patients. *Eur J Nucl Med.* 1993;20:716–731.
8. Froidevaux S, Eberle AN. Somatostatin analogs and radiopeptides in cancer therapy. *Biopolymers.* 2002;66:161–183.
9. Eberle AN. Proopiomelanocortin and the melanocortin peptides. In: Cone RD, ed. *The Melanocortin Receptors.* Totowa, NJ: Humana Press, Inc.; 2000:3–67.
10. Balch CM, Soong SJ, Murad TM, Smith JW, Maddox WA, Durant JR. A multifactorial analysis of melanoma. IV. Prognostic factors in 200 melanoma patients with distant metastases (stage III). *J Clin Oncol.* 1983;1:126–134.
11. Chen J, Cheng Z, Hoffman TJ, Jurisson SS, Quinn TP. Melanoma-targeting properties of ^{99m}technetium-labeled cyclic alpha-melanocyte-stimulating hormone peptide analogues. *Cancer Res.* 2000;60:5649–5658.
12. Miao Y, Owen NK, Whitener D, Gallazzi F, Hoffman TJ, Quinn TP. In vivo evaluation of ^{188}Re-labeled alpha-melanocyte stimulating hormone peptide analogs for melanoma therapy. *Int J Cancer.* 2002;101:480–487.
13. Froidevaux S, Calame-Christe M, Tanner H, Sumanovski L, Eberle AN. A novel DOTA-α-melanocyte-stimulating hormone analog for metastatic melanoma diagnosis. *J Nucl Med.* 2002;43:1699–1706.
14. Cheng Z, Chen J, Miao Y, Owen NK, Quinn TP, Jurisson SS. Modification of the structure of a metallopeptide: synthesis and biological evaluation of ^{111}In-labeled DOTA-conjugated rhenium-cyclized alpha-MSH analogues. *J Med Chem.* 2002; 45:3048–3056.
15. Chen J, Cheng Z, Owen NK, et al. Evaluation of an ^{111}In-DOTA-rhenium cyclized alpha-MSH analog: a novel cyclic-peptide analog with improved tumor-targeting properties. *J Nucl Med.* 2001;42:1847–1855.
16. Mariani G, Bodei L, Adelstein SJ, Kassis AI. Emerging roles for radiometabolic therapy of tumors based on auger electron emission. *J Nucl Med.* 2000;41:1519–1521.
17. Sahm UG, Olivier GW, Branch SK, Moss SH, Pouton CW. Synthesis and biological evaluation of alpha-MSH analogues substituted with alanine. *Peptides.* 1994;15:1297–1302.
18. Fidler IJ. Selection of successive tumour lines for metastasis. *Nat New Biol.* 1973;242:148–149.
19. Froidevaux S, Eberle AN. Homologous regulation of melanocortin-1 receptor (MC1R) expression in melanoma tumor cells in vivo. *J Recept Signal Transduct Res.* 2002;22:111–121.
20. Schuhmacher J, Maier-Borst W. A new Ge-68/Ga-68 radioisotope generator system for production of Ga-68 in dilute HCl. *Int J Appl Radiat Isot.* 1981;32: 31–36.
21. Doll J, Zaers J, Trojan H, et al. Optimization of PET image quality by means of 3D data acquisition and iterative image reconstruction. *Nuklearmedizin.* 1998; 37:62–67.
22. Mijnhout GS, Hoekstra OS, van Tulder MW, Teule GJ, Deville WL. Systematic review of the diagnostic accuracy of ^{18}F-fluorodeoxyglucose positron emission tomography in melanoma patients. *Cancer.* 2001;91:1530–1542.
23. Dimitrakopoulou-Strauss A, Strauss LG, Burger C. Quantitative PET studies in pretreated melanoma patients: a comparison of 6-[^{18}F]fluoro-L-dopa with ^{18}F-FDG and ^{15}O-water using compartment and noncompartment analysis. *J Nucl Med.* 2001;42:248–256.
24. Cutler CS, Smith CJ, Ehrhardt GJ, Tyler TT, Jurisson SS, Deutsch E. Current and potential therapeutic uses of lanthanide radioisotopes. *Cancer Biother Radiopharm.* 2000;15:531–545.
25. Kozak RW, Raubitschek A, Mirzadeh S, et al. Nature of the bifunctional chelating agent used for radioimmunotherapy with ^{90}Y monoclonal antibodies: critical factors in determining in vivo survival and organ toxicity. *Cancer Res.* 1989;49:2639–2644.
26. Froidevaux S, Eberle AN, Christe M, et al. Neuroendocrine tumor targeting: study of novel gallium-labeled somatostatin radiopeptides in a rat pancreatic tumor model. *Int J Cancer.* 2002;98:930–937.
27. Ugur O, Kothari PJ, Finn RD, et al. Ga-66 labeled somatostatin analogue DOTA-DPhe1-Tyr3-octreotide as a potential agent for positron emission tomography imaging and receptor mediated internal radiotherapy of somatostatin receptor positive tumors. *Nucl Med Biol.* 2002;29:147–157.
28. Deen WM, Satvat B, Jamieson JM. Theoretical model for glomerular filtration of charged solutes. *Am J Physiol.* 1980;238:F126–F139.
29. Christensen EI, Rennke HG, Carone FA. Renal tubular uptake of protein: effect of molecular charge. *Am J Physiol.* 1983;244:F436–F441.
30. Lawrence GM, Brewer DB. Glomerular ultrafiltration and tubular reabsorption of bovine serum albumin and derivatives with increased negative charge in the normal female Wistar rat. *Clin Sci.* 1984;66:47–54.
31. Kok RJ, Haas M, Moolenaar F, de Zeeuw D, Meijer DK. Drug delivery to the kidneys and the bladder with the low molecular weight protein lysozyme. *Ren Fail.* 1998;20:211–217.
32. Akizawa H, Arano Y, Mifune M, et al. Effect of molecular charges on renal uptake of ^{111}In-DTPA-conjugated peptides. *Nucl Med Biol.* 2001;28:761–768.
33. Vaidyanathan G, Zalutsky MR. Fluorine-18-labeled [Nle^{4},D-Phe^{7}]-alpha-MSH, an alpha-melanocyte stimulating hormone analogue. *Nucl Med Biol.* 1997;24: 171–178.
34. Bagutti C, Stolz B, Albert R, Bruns C, Pless J, Eberle AN. [^{111}In]-DTPA-labeled analogues of alpha-melanocyte-stimulating hormone for melanoma targeting: receptor binding in vitro and in vivo. *Int J Cancer.* 1994;58:749–755.
35. Heppeler A, Froidevaux S, Mäcke HR, et al. Radiometal labelled macrocyclic chelator derivatised somatostatin analogue with superb tumour targeting properties and potential for receptor mediated internal radiotherapy. *Chem Eur J.* 1999;5:1016–1023.
36. de Jong M, Rolleman EJ, Bernard BF, et al. Inhibition of renal uptake of indium-111-DTPA-octreotide in vivo. *J Nucl Med.* 1996;37:1388–1392.
37. de Jong M, Breeman WA, Bernard BF, et al. [^{177}Lu-DOTA^{0},Tyr^{3}]octreotate for somatostatin receptor-targeted radionuclide therapy. *Int J Cancer.* 2001;92:628–633.
38. de Jong M, Breeman WA, Bernard BF, et al. Tumour uptake of the radiolabelled somatostatin analogue [DOTA^{0},Tyr^{3}]octreotide is dependent on the peptide amount. *Eur J Nucl Med.* 1999;26:693–698.